Implications of the differences between daytime and nighttime CloudSat observations over the tropics

Chuntao Liu, Edward J. Zipser, Gerald G. Mace, and Sally Benson

Department of Meteorology, University of Utah

Submitted to Journal of Geophysical Research – Atmospheric Sciences in Jan, 2008

Revised in Mar, 2008

Jan 2008

Key words: CloudSat, TRMM, tropical precipitation, clouds, diurnal cycle

Corresponding author address: Dr. Chuntao Liu, Department of Meteorology, University of Utah, 135 S 1460 E Rm. 819, Salt Lake City, UT, 84112-0110

Email: liu.c.t@utah.edu

Abstract

Using one year of CloudSat level 2B Cloud Geometrical Profile product, the vertical structures, geographical distributions and seasonal variations of cloud occurrence at the day time (1330 LT) and the night time (0130 LT) overpasses and their differences over tropical land and ocean are presented separately. The differences between the cloud and precipitation occurrence at 0130 and 1330 and the 24 hour mean are quantitatively evaluated using climatologies of diurnal variation from 9 years of TRMM observations. Then the vertical structures, geographical distributions and seasonal variations of cloud and precipitation near the two CloudSat overpass times are generated from 9 years of TRMM observations and compared to those from CloudSat. Larger differences between cloud and precipitation occurrences at 0130 and those at 1330 were found at high altitudes because the amplitude of diurnal variation increases with height. Cloud and precipitation occurrences show day vs. night differences which are opposite with respect to each other in the upper troposphere over the tropics. For example, near 1330 LT over tropical oceans, there are more clouds, but less precipitation at 13-14 km than near 0130 LT except over Panama. This may be explained with the phase lags between precipitation and clouds in the life cycles of the convective systems over land and ocean. The differences between the seasonal cycles of cloud and precipitation sampled at the 0130 and 1330 A-Train overpass times and the seasonal cycles generated from full day samples are shown.

1. Introduction

As an important member of the A-Train satellites [Stephens et al., 2002], CloudSat has provided valuable observations of clouds and precipitation globally since its April 2006 launch [Haynes et al., 2007; Mace et al., 2007; Zhang et al., 2007]. Like other A-Train satellites, CloudSat's sun-synchronous orbit passes over the tropics near 0130 and 1330 local time (LT). It is well known that there are strong diurnal cycles of precipitation and clouds over the tropics [e.g., Gray and Jacobson 1977, Augustine, 1984, Janowiak et al., 1994; Hall and Vonder Haar, 1999; Yang and Slingo, 2001; Dai, 2001; Dai et al., 2007]. Due to observations from the Tropical Rainfall Measuring Mission (TRMM, Kummerow et al., 1998), the diurnal variations of cloud and precipitation properties and vertical structure are known in greater detail [Imaoka and Spencer, 2000; Sorooshian et al, 2002; Nesbitt and Zipser 2003; Liu and Zipser 2008]. Due to the diurnal cycles of clouds and precipitation, large differences between the CloudSat daytime (1330) and nighttime (0130) observations are expected. In addition to finding explanations for these differences, a more immediate question is how different the climatologies of precipitation and clouds generated from the CloudSat observations are from climatologies produced from full day samples.

An example of the climatology of diurnal variation of tropical precipitation echoes from TRMM [Liu and Zipser, 2008] is shown in Figure 1. Over tropical land, the A-Train satellites do not capture the strongest or most frequent afternoon convective period

(Figure 1a). Over tropical oceans, the early morning precipitation maximum is also not captured (Figure 1b). Because the amplitude of the diurnal cycle of precipitation increases with height over both tropical land and ocean, the differences between the daytime and night time precipitation observations of CloudSat are expected to be larger at higher altitudes. Therefore, if observations from CloudSat and other A-Train Satellites are to be used to understand the role of clouds and precipitation in the diabatic heating of the atmosphere, it is important to understand the implications of the sub-sampling of the full diurnal cycles.

In this study, we focus on presenting and interpreting the differences between the daytime and nighttime observations from CloudSat over the tropics. The questions addressed include:

- What are the differences from the climatologies of total amount of cloud and precipitation of CloudSat, which samples only at two specific times of the day, to the climatologies from the full day?
- What are the differences of CloudSat observed clouds and precipitation between day and night over the tropics? How may we interpret these differences?
- What are the seasonal cycles of CloudSat-observed clouds and precipitation observed during the daytime and the night time? Are they similar? How different are they from the seasonal cycles generated from the TRMM full day samples?

First TRMM observations at A-Train observation times are compared with the full day sample of TRMM observations. Then day-night differences of vertical structure, geographical and seasonal distributions of cloud and precipitation from CloudSat over the

tropics are presented. Next we interpret these differences by using the climatologies of diurnal variation of cloud and precipitation generated from 9 years of TRMM observations.

2. Data and methods

2.1 CloudSat data

One full year (July 2006 to June 2007) of CloudSat level 2B Cloud Geometrical Profile (2B-GEOPROF) data [Mace, 2007; Marchand et al., 2007] is used in this study. In the CloudSat Profiling Radar (CPR) [Im et al., 2006] reflectivity, clouds are identified with a cloud mask. In this study, CloudSat observations flagged as significant with the CloudSat cloud mask [Marchand et al., 2007] and CPR reflectivity greater than -20 dBZ are considered as cloud (hereafter referred to as cloudy pixels). Pixels with CPR reflectivity greater than 0 dBZ are considered as thick cloud with precipitation particles (referred to as precipitation from now on). The occurrence frequencies of cloud and precipitation are presented vertically, geographically, and seasonally over the tropics from 20^{o}S-20^{o}N.

To calculate these frequencies, the total number of sampled pixels (cloudless and cloudy), and total number of cloud and precipitation pixels, and the total number of pixels with a reflectivity greater than or equal to the thresholds of -20, -10, 0, and 10 dBZ are accumulated monthly into 1 km bins from 0 to 20 km in 1^{o}x1^{o} boxes globally from daytime and nighttime observations separately. Then the vertical profiles of occurrence

frequency of cloudy pixels and a reflectivity greater than or equal to -20, -10, 0 and 10 dBZ are calculated by dividing the accumulated cloudy and precipitation pixels with the total sampled pixels in the boxes for daytime and nighttime over land and oceans in the tropics, separately. The geographical distributions of the occurrences of precipitation pixels and reflectivity greater than or equal to 10 dBZ are generated by summarizing the occurrences on a $5^o \times 5^o$ grid.

2.2 TRMM data

The TRMM satellite has a non-sun-synchronous 35^o inclination orbit covering the tropics and subtropics, with instruments for observing precipitation, clouds, and lightning [Kummerow et al, 1998]. Given enough observation time, TRMM data provides detailed information about the diurnal cycles of precipitation and clouds [Negri et al., 2002; Nesbitt and Zipser, 2003; Liu and Zipser, 2008]. This study uses the TRMM Precipitation and Cloud Feature (PF) database created from 9 years of TRMM observations. The database includes more than one hundred million PFs defined by grouping the near surface raining area observed by the TRMM Precipitation Radar (PR), area projected from the pixels with PR 20 dBZ, or cloud area with the Visible Infrared Scanner (VIRS) 10.8 μm brightness temperature (T_{B11}) colder than 235 K [Liu et al., 2008]. For each one of these PFs, the area of 20 dBZ at different altitudes, area of cloud with $T_{B11} < 210$ K and 235 K, and flash counts are summarized. Here we present the occurrence of precipitation, clouds colder than 210 K and 235 K, and lightning flash counts at the A-Train observation times and their contributions to the full day average.

3. Results and discussion

3.1 Occurrence of TRMM precipitation and cloud at A-Train observation times

Before presenting the differences between daytime and nighttime CloudSat observations, it is important to know the contribution of precipitation and clouds at the A-Train observing times compared to the full day average. By dividing the TRMM precipitation occurrence at 0100-0200 and 1300-1400 by the 24-hour mean, the deviation of the precipitation occurrences at the A-Train times from the mean at different altitudes are calculated and shown in Figure 2. Over tropical land (Figure 2a), precipitation occurs more frequently during the day time and less frequently during the night overpasses than the mean above 8 km. During the day the discontinuity at mid-levels from 5 to 8 km matches up well with the discontinuity at mid-levels in Figure 1a. Below 5 km, precipitation at both overpass times occurs more frequently than the mean. The averaged precipitation occurrence from the day and night observations is about 10% more than the mean below 2 km, and 20% less than the mean above 14 km. Over tropical oceans (Figure 2b), precipitation occurs more frequently during the night and less frequently during the day time overpasses than the mean. The deviations from the mean at both day time and night time are near 0 at 5 km, but up to 35% at high altitudes. However, the average of precipitation occurrences from the two CloudSat overpass times is very close to the 24-hour mean with about 5% overestimation above 8 km.

153 TRMM observations also provide information on the diurnal cycles of clouds and
154 lightning [Liu and Zipser, 2008]. By dividing the 9 years of TRMM observations of near
155 surface volumetric rain, clouds with T_{B11} < 210 K and 235 K, population of PFs, and
156 flash counts at 0100-0200 and 1300-1400 by the 24-hour mean, the deviations of the total
157 precipitation, occurrence of cold clouds, population of precipitation systems and flashes
158 at A-Train times from the mean are calculated and listed in Table 1. Over land, there are
159 larger populations of PFs with more flashes and with larger volumetric rainfall, but fewer
160 clouds colder than 210 K and 235 K in the day time than at night. This can be explained
161 by the phase lags of the diurnal cycles of the convective systems over land [Hong et al.,
162 2006; Liu and Zipser, 2008]. At 1330, most of the convective systems are still in the
163 developing stage and have high flash rates, high rainfall intensity, but do not have large
164 areas of cold clouds. However, at 0130, most of the convective systems over land have
165 completed their life cycles, but large areas of cold clouds generated by a small number of
166 long-lived mesoscale convective systems (MCSs) may still exist. Over ocean, there are
167 more PFs with more rainfall, clouds with T_{B11} < 210 K and flashes at the night time
168 overpasses than the mean, and fewer PFs with less rainfall, clouds with T_{B11} < 210 K and
169 flashes at the day time overpasses than the mean. The only exception is the area of clouds
170 with T_{B11} < 235 K, which is greater during the day. This may be an effect of daytime
171 cirrus clouds. After averaging both the day and the night data, the values of near surface
172 volumetric rain, cold clouds, and population of PFs are close to the mean, with less than
173 5% overestimation.
174

The geographical distribution of the ratio of the occurrence of PR 20 dBZ at 14 km and VIRS T_{B11} < 235 K at the 1300-1400, 0100-0200 observation times and their average to the mean of all day samples is shown in Figure 3. Large fractional differences from the occurrence of PR 20 dBZ at 14 km at day time and night time to the mean of full day samples are obvious over central Africa and the Amazon in Figure 3a and 3b. The average occurrence of the day time and night time values is greater than the mean of full day samples over most of the Amazon and Southern Africa, but less than the mean over the Sahel (Fig 3c). Consistent with Figure 2b, the Tropical Ocean has a large area with higher occurrence of 20 dBZ at 14 km at night time than the mean of full day samples. Generally there are fewer clouds colder than 235 K over tropical land at both day time and night time than the mean of full day samples (Figure 3d, 3e). Even though the average of the day time and night time occurrences of cloud colder than 235 K over the entire tropical ocean is only about 4% different from the mean of full day samples (Table 1), there are some regional variations shown in Figure 3f. The day time and night time average is larger than the mean over most of the Atlantic and the East Pacific, but less than the mean over about half of the West Pacific and the Indian Ocean.

3.2 Cloud and precipitation vertical structure from CloudSat

The daytime and night time vertical profiles of the occurrence of CloudSat CPR pixels with cloud mask, -20, -10, 0, and 10 dBZ, as well as the occurrence of TRMM PR 20 dBZ at 0100-0200 and 1300-1400 with a vertical bin size of 1 km are shown for land and ocean separately in Figure 4a and 4b. The ratio of the occurrence during the daytime to

198 the occurrence during the nighttime from Figure 4 is shown in Figure 5. The low
199 occurrence of the CPR 10 dBZ below the melting level in Figure 4a and 4b is due to radar
200 attenuation. In Figure 4a, CloudSat detects more clouds at 10-13 km than other altitudes
201 during both day and night over land. Clouds and precipitation occur more frequently in
202 the day time below 3 km. In the mid troposphere (4-8 km), up to a 20 % higher
203 occurrence of clouds and high reflectivity exists during the night than during the day
204 (Figure 4a, 5a). In the upper troposphere (9-12 km), clouds (< -10 dBZ) happen more
205 frequently during the night, but precipitation (> 0 dBZ) happens more frequently during
206 the day (Figure 4a, 5a). In the day, most of the convective systems over land are in an
207 early development stage. There is more shallow precipitation, and more clouds with high
208 reflectivity reaching high altitudes in deep convective cells [Liu and Zipser, 2005]. In the
209 night, most of the convective systems that remain are in the dissipating stage, or are large
210 MCSs with large stratiform fractions. There is much less deep convection [Nesbitt and
211 Zipser, 2003].
212
213 Over ocean, more clouds are detected below 2 km and at 10-13 km than at other altitudes
214 by the CPR (Figure 4b). More clouds and precipitation are below 7 km during the night
215 than during the day. However, more cloud pixels (including those < -10 dBZ), but less
216 thick precipitating cloud pixels (> 0 dBZ) are above 10km during the day than at night. It
217 seems possible that the greater occurrence of daytime high clouds can be residual cirrus
218 clouds with low reflectivity (< 10 dBZ) from early morning convection. However, diurnal
219 cycles of precipitation and clouds over tropical oceans may include contributions from
220 nocturnal convection, early morning convective showers, and shallow early afternoon

showers [Sui et al., 1997; Pereira and Rutledge, 2006; Liu and Zipser, 2008]. It may be premature to explain the differences between the day and night time cloud and precipitation statistics as a simple function of the life cycles of the early morning convective systems, thus further investigation is warranted.

3.3 Geographical variation

Several studies have shown the geographical distribution of clouds from CloudSat [e.g., Mace et al., 2007]. Here we focus on the differences between the CloudSat CPR detected clouds and precipitation with reflectivity greater or equal to 10 dBZ in the upper tropical troposphere at 13-14 km during the 1330 and 0130 observation times. As shown in Figure 6a, 6b and 6e, precipitation is more frequent over the ocean at 0130 and over land at 1330 at 13-14 km. Figure 6c, 6d and 6f show that high clouds occur more frequently over the west Pacific, Africa, Panama, and Amazon at both 1330 and 0130 observation times. Consistent with Figure 4, in general high clouds are more frequent over the ocean at 1330 and over land at 0130. The most noticeable exception is over Panama, where there are more high clouds during the day, but more precipitation at night.

For comparison, the occurrences of TRMM 20 dBZ at 14 km and cloud with $T_{B11} < 235$ K during 0100-0200 and 1300-1400 and their differences are shown in Figure 7. The geographical distributions of precipitation from the TRMM PR and cloud from infrared images in Figure 7a-d are close to those shown in Figure 6a-d, with the exception that TRMM PR 20 dBZ occurs less frequently over ocean than CPR 10 dBZ. The patterns of the differences between the day time and the night time precipitation with TRMM PR >

20 dBZ at 14 km in Figure 7e and cold clouds in Figure 7f are consistent with Figure 6e and 6f, including the exception over Panama.

3.4 Seasonal variation

Large deviations between the amounts of precipitation and clouds observed at the A-Train observation times and the amounts from the full day average were shown in section 3.1. In this section we try to show how different the seasonal cycles of precipitation and clouds sampled at A-Train times are from the seasonal cycle from the full day samples. The normalized seasonal variation of the occurrence of CloudSat CPR cloud and precipitation with 10 dBZ or greater at 13-14 km over tropical land and ocean are shown in Figure 8a-d. There are some differences between the seasonal variation of the high clouds and precipitation at 1330 and those from the seasonal variations at 0130. Over land, large differences occur in July-August, due to a larger contribution of high cloud at 0130. In November there is a larger contribution of high cloud at 1330 (Figure 8a and 8c). Over ocean, the seasonal variation of high clouds at 1330 and at 0130 show large differences in July and October (Figure 8b and 8d).

For comparison, the seasonal variations of the occurrence of TRMM PR 20 dBZ at 14 km, and cloud with VIRS T_{B11} 235 K at 0100-0200 and 1300-1400 are shown in Figure 9. Due to interannual variability, some differences between the seasonal variation of cloud and precipitation from the 9 year TRMM database in Figure 9 and those from 1 year of

CloudSat data in Figure 8 are to be expected. Here we focus on the differences between the seasonal cycles of cloud and precipitation generated from the daytime and the night time. The differences between the daytime and the night time high clouds from TRMM VIRS in Figure 9a-d closely resemble the patterns of the differences from the CloudSat observations as shown in Figure 8a-d. It is important to note that neither the seasonal cycles of high clouds at 1330 nor at 0130 can well represent the seasonal cycle derived from the mean of full day samples (thick gray line in Figure 9), especially over tropical oceans (Figure 9b and 9d). This suggests large seasonal variations in the diurnal cycles of cloud and precipitation over some parts of the Tropics.

As shown in Figure 10, the day to night ratios of cloud and precipitation occurrence vary seasonally at different altitudes. This is caused by the seasonal variation of the amplitude or phase of the diurnal cycles of cloud and precipitation. Consistent with Figure 4a and 5a, precipitation over land occurs more frequently at the daytime and clouds occur more frequently at the night time at 10-13 km during most of the year with the exception that both clouds and precipitation occur more frequently during the night in July and August at these levels. Large differences among the vertical structures of day vs. night ratios of occurrence of CPR pixels with cloud mask, -10 dBZ and 10 dBZ exist over the ocean. Consistent with Figure 8b, May, July and October (Figure 10f) show large day vs. night differences in clouds and precipitation. Further investigations of these variations are needed to properly interpret the day-night seasonal differences of clouds.

3.5 Sample size

290 Because only one year of CloudSat data is used in the above discussion, a large enough
291 sample size is important for the robustness of the statistics. This discussion focuses on the
292 sample size of the geographical distribution of cloud and precipitation occurrence shown
293 in Figure 6 and 7 because it has a smaller sample size than the seasonal and vertical
294 distributions shown in Figure 4, 5, 8 and 9.
295
296 The mean of the total number of sampled columns in a $5^{o}\times5^{o}$ box in 20^{o}S-20^{o}N from one
297 year of CloudSat data is approximately 37,500. Since pixels are accumulated in each
298 column at a 1 km vertical interval, and considering each CloudSat column has a ~ 240 m
299 vertical resolution, more than 150,000 pixel samples are in a $5^{o}\times5^{o}$ box at each 1 km
300 vertical interval. A CPR cloud or precipitation pixel represents $\sim6.6\times10^{-6}$ fractional
301 occurrence. This is at least three orders of magnitude lower than the occurrences shown
302 in Figure 6a, b, and e, and about four orders of magnitude lower than the occurrences
303 shown in Figure 6c, d, and f. Therefore, the fractional occurrences shown in Figure 6 are
304 in no way near the margins of sampling.
305
306 Compared to the CloudSat CPR, the TRMM PR samples about four times less frequently
307 along the orbit due to its larger footprint, although it samples 49 times more frequently at
308 each scan across the orbit swath. Since only 1/24 of the samples are used to match
309 CloudSat overpass times, even with 9 years of TRMM PR data, only ~ 670,000 samples
310 are in a $5^{o}\times5^{o}$ box in Figure 7. A pixel with 20 dBZ represents about 1.5×10^{-6} fractional
311 occurrence. This is about two orders of magnitude lower than those shown in Figure 7a, b,
312 and e, and four orders of magnitude lower than those shown in Figure 7c, d and f. To

avoid regions with marginal sample size, the occurrence differences in Figure 7e and Figure 3a-c are only shown for boxes with at least 10 pixels of 20 dBZ.

In Figure 9, we did not use seasonal cycles from the same time period of TRMM PR data as CloudSat. This is because there would be serious diurnal sampling biases if we subsample at CloudSat overpass times from only a month of TRMM PR data to generate the seasonal cycles [Negri et al., 2002; Fisher, 2007].

4. Summary

- Substantial differences in the climatologies of cloud and precipitation sampled at the A-Train overpass times exist when compared to the daily average climatologies. The difference is larger over land than over ocean, especially at higher altitudes where the diurnal cycle has larger amplitudes.
- Cloud and precipitation show different day vs. night occurrence frequencies in the upper troposphere over tropical land and ocean at A-Train overpass times. High clouds are found to occur much more frequently during the daytime overpass time. This may be due to the phase lags between precipitation and clouds in the life cycles of the convective systems over land and ocean.
- There are differences between the seasonal cycles of cloud and precipitation over the tropics sampled at 0130 and those sampled at 1330. Simulation of sampling at A-Train overpass times using TRMM data suggests that the seasonal variations of clouds sampled at A-Train overpass times are different from the seasonal cycles of clouds

derived from full day averages. This may be explained by the seasonal variation of the diurnal cycles over tropics.

These results suggest the importance of interpreting the CloudSat and other A-Train observations at 1330 and 0130 as independent samples at their respective times within the diurnal cycle. This is especially important if the data are to be used for climate model validation. Unfortunately, most climate models currently generate output statistics only every 3 hours. It is clear that the vertical structure of precipitation and clouds vary significantly on this time scale (Figure 1). Therefore, it is important that models are sampled in ways that account for the physical processes that drive the diurnal cycle of the tropical atmosphere if comparisons to observations are to be beneficial.

Acknowledgement

This research was supported by NASA Precipitation Measurement Mission grants NAG5-13628 and NN-H-06-Z-DA-001-N under the direction of Dr. Ramesh Kakar. A portion of this work was also supported by the Jet Propulsion Laboratory, California Institute of Technology, sponsored by the National Aeronautics and Space Administration. Special thanks go to Drs. Erich Stocker and John Kwiatkowski and the rest of the TRMM Science Data and Information System (TDSIS) at NASA Goddard Space Flight Center, Greenbelt, MD, for data processing assistance.

356 References

357

358 Augustine, J. A., The diurnal variation of large-scale inferred rainfall over the tropical
359 Pacific Ocean during August 1979, *Mon. Wea. Rev.*, **112**, 1745-1751, 1984.
360 Dai, A., Global precipitation and thunderstorm frequencies. Part II: Diurnal variations, *J.*
361 *Climate*, **14**, 1112-1128, 2001.
362 Dai, A., X. Lin, and K. Hsu, The frequency, intensity, and diurnal cycle of precipitation
363 in surface and satellite observations over low- and mid-latitudes, *Clim. Dyn.*, **29**, doi
364 10.1007/s00382-007-0260-y, 2007.
365 Fisher, B., Statistical error decomposition of regional-scale climatological precipitation
366 estimates from the Tropical Rainfall Measureing Mission (TRMM), *J. App. Meteor.*
367 *Clim.*, **46**, 791-813, doi:10.1175/JAM2497, 2007.
368 Gray, W. M., and R. W. Jacobson, Diurnal variation of deep cumulus convection, *Mon.*
369 *Wea. Rev.*, **105**,1171-1188, 1977.
370 Hall, T. J., and T. H. Vonder Haar, The diurnal cycle of west Pacific deep convection and
371 its relation to the spatial and temporal variation of tropical MCSs, *J. Atmos. Sci.*, **56**,
372 3401-3415, 1999.
373 Haynes, J. M., and G. L. Stephens, Tropical oceanic cloudiness and the incidence of
374 precipitation: early results from CloudSat, *Geophys. Res. Lett.*, **34**, L09811,
375 doi:10.1029/2007GL029335, 2007.
376 Hong, G., G. Heygster, C. A. Rodriguez, Effect of cirrus clouds on the diurnal cycle of
377 tropical deep convective clouds, *J. Geophys. Res.*, **111**, D06209,
378 doi:10.1029/2005JD006208, 2006.

379 Im, E., et al., Cloud profiling radar for the CloudSat misstion, *IEEE Trains. Aerosp.*
380 *Electron. Syst.*, **20**, 15-18, 2006.
381 Imaoka, K. and R. W. Spencer, Diurnal variation of precipitation over the tropical oceans
382 observed by TRMM/TMI combined with SMM/I, *J. Climate*, **13**, 4149-4158, 2000.
383 Janowiak, J., P. A. Arkin, and M. Morrissey, An examination of the diurnal cycle in
384 oceanic tropical rainfall using satellite and in situ data. *Mon. Wea. Rew.*, **122**, 2296-
385 2311, 1994.
386 Kummerow, C., W. Barnes, T. Kozu, J. Shiue, and Joanne Simpson, The Tropical
387 Rainfall Measuring Mission (TRMM) Sensor Package. *J. Atmos. Oceanic Tech.*, **15**,
388 809–817, 1998.
389 Liu, C., and E. Zipser, Global distribution of convection penetrating the tropical
390 tropopause, *J. Geophys. Res.*, doi:10.1029/2005JD00006063, 2005.
391 Liu, C., E. Zipser, D. Cecil, S. W. Nesbitt, and S. Sherwood, A cloud and precipitation
392 feature database from 9 years of TRMM observations, submitted to *J. Appl. Meteor.*
393 *Climate.*, 2008.
394 Liu. C., E. Zipser, Diurnal cycles of precipitation, clouds and lightning in the tropics from
395 9 years of TRMM observations, *Geophys. Res. Lett.*, **35**, L04819,
396 doi:10.1029/2007GL032437, 2008.
397 Mace, G. G., R. Marchand, Q. Zhang, and G. Stephens, Global hydrometeor occurrence
398 as observed by CloudSat: Initial observations from summer 2006, *Geophys. Res.*
399 *Lett.*, **34**, L0908, doi:10.1029/2006GL029017, 2007.

Marchand, R., Mace, G. G., Ackerman, T., and Stephens, G., Hydrometeor detection using CloudSat – An Earth observing 94GHz cloud radar, accepted, *J. Atmos. Ocean. Tech.*, 2007.

Negri, A. J., T. L. Bell, and L. Xu, Sampling of the diurnal cycle of precipitation using TRMM, *J. Atmos. Ocean. Tech.*, **19**, 1333-1344, 2002.

Nesbitt, S. W., and E. J. Zipser, The diurnal cycle of rainfall and convective intensity according to three years of TRMM measurements. *J. Climate*, **16**, 1456-1475, 2003.

Pereira, L. G., and S. A. Rutledge, Diurnal cycle of shallow and deep convection for a tropical land and ocean environment and its relationship to synoptic wind regimes, *Mon. Wea. Rev.*, **134**, 2688-2701, 2006.

Sorooshian, S., X. Gao, K. Hsu, R. A. Maddox, Y. Hong, H. V. Gupta, and B. Imam, Diurnal variability of tropical rainfall retrieved from combined GOES and TRMM satellite information, *J. Climate*, **15**, 983-1001, 2002.

Stephens, G. L., et al., The CloudSat missiton and the A-Train, *Bull. Am. Meteorol., Soc.*, **83**, 1771-1790, 2002.

Sui, C.-H., K. M. Lau, Y. N. Takayabu, and D. A. Short, Diurnal variations in tropical oceanic cumulus convection during TOGA COARE. J. Atmos. Sci., 54, 639-655, 1997.

Yang, G.-Y, and J. Slingo, The diurnal cycle in the tropics, *Mon. Wea. Rew.*, **129**, 784-801, 2001.

Yuter, S. E., and R. A. Houze, Three-dimensional kinemetic and microphysical evolution of Florida cumulonimbus. Part II: Frequency distributions of vertical velocity, reflectivity, and differential reflectivity, *Mon. Wea. Rev.*, **123**, 1941-1963, 1995.

423 Zhang, Y., S. Klein, G. G. Mace, and J. Boyle, Gluster analysis of tropical clouds using
424 CloudSat data, *Geophys. Res. Lett.*, **34**, L12813, doi:10.1029/2007GL029336, 2007.
425

Figure Captions:

Figure 1. Contoured Frequency-by-Altitudes Diagrams (CFADs) of diurnal variation of precipitation area with TRMM PR reflectivity greater than or equal to 20 dBZ over 20^oS-20^oN land (a) and ocean (b). Units are in %. Vertical dashed lines are the A-Train satellite observations around 0130 and 1330 local time.

Figure 2. Percentage differences from occurrence of TRMM PR 20 dBZ around the A-Train observing day time (0100-0200) and the night time (1300-1400) to the all day mean occurrence over 20^oS-20^oN land (a) and ocean (b).

Figure 3. a) Ratio of the occurrence of TRMM PR 20 dBZ at 14 km at 1300-1400 to the mean from 9 years of full day samples, only shown for $5^o \times 5^o$ boxes with at least 10 pixels with 20 dBZ. b) same as a), but for occurrence at 0100-0200. c) same as a) but for occurrence of averaging 0100-0200 and 1300-1400, only shown for $5^o \times 5^o$ boxes with at least 10 pixels with 20 dBZ at both 1300-1400 and 0100-0200. d) Ratio of the occurrence of TRMM VIRS $T_{B11} < 235$ K at 1300-1400 to the mean from all day samples, only shown for $5^o \times 5^o$ boxes with at least 10000 pixels with $T_{B11} < 235$ K. e) same as d), but for ratio of occurrence at 0100-0200 to the mean. f) same as d) but for ratio of occurrence of averaging 0100-0200 and 1300-1400 to the mean.

Figure 4. Occurrence (fraction) of sampled pixels with cloud mask, -20, -10, 0, 10 dBZ observed by CloudSat CPR and 20 dBZ observed by TRMM PR at different altitudes over tropical land (a) and ocean (b) (20^oS-20^oN) at the A-Train day (1330) and night (0130) observation times. Here TRMM PR occurrences are summarized from the observations during 0100-0200 and 1300-1400 local time. The vertical bin

size is 1 km. Light blue (yellow) filled areas indicate differences when night time occurrence is greater (less) than that of day time.

Figure 5. Ratios from the daytime to the night time CPR and PR reflectivity occurrences over land (a) and ocean (b) in Figure 3.

Figure 6. a) Occurrence (fraction) of CloudSat CPR reflectivity greater or equal to 10 dBZ at 13-14 km at night time. b) Same as a) but for day time. c) Occurrence of clouds detected by CloudSat CPR at 13-14 km at night time. d) Same as c) but for day time. e) Differences between day time and night time CPR 10 dBZ occurrences restricted to $5^o \times 5^o$ boxes with at least 1000 pixels with 10 dBZ in both a) and b). f) Differences between day time and night time CPR cloud occurrences restricted to $5^o \times 5^o$ boxes with at least 1000 pixels with cloud mask in both c) and d).

Figure 7. a) Occurrence of TRMM PR reflectivity greater or equal to 20 dBZ at 14 km for night time (0100-0200). b) same as a) but for day time (1300-1400). c) Differences between day time and night time. d) Occurrence of TRMM VIRS $T_{B11} < 235$ K for night time (0100-0200). e) Differences (a)-(b) between day time and night time occurrence of PR 20 dBZ at 14 km restricted to $5^o \times 5^o$ boxes with at least 10 pixels of 20 dBZ in both a) and b). f) Differences between day time and night time occurrence of cloud colder than 235 K restricted to $5^o \times 5^o$ boxes with at least 1000 pixels of cloud colder than 235 K in both a) and b).

Figure 8. Seasonal variation of occurrence of CloudSat CPR clouds (c and d) at 13-14 km and occurrence of CPR 10 dBZ (a and b) at 13-14 km over tropical land and ocean ($20S^o$-$20N^o$). The mean values for month 1-6 are from data in 2007, and the mean values for month 7-12 are from data in 2006.

Figure 9. Seasonal variation of area of PR 20 dBZ reaching 14 km (a and b), and T_{B11} < 235 K (c and d) from all the TRMM observations and from only the TRMM observations during 0100-0200 and 1300-1400 local time over tropical land and ocean (20^{o}S-20^{o}N).

Figure 10. Seasonal variation of ratios of occurrences of CloudSat cloud, CPR reflectivity > -10 dBZ, > 10 dBZ in the daytime to those at night over land and ocean. The mean values for month 1-6 are from data in 2007, and mean values for month 7-12 are from data in 2006.

Table 1. Percentage deviation of the TRMM precipitation volume, area of cold clouds, flashes and population of precipitation systems at 0100-0200 and 1300-1400 from the mean over tropics (20^{o}S-20^{o}N).

	Land			Ocean		
	Day	Night	Average	Day	Night	Average
Population of PFs	58	-18	20	-10	16	3
Volumetric rain	29	-5	12	-6	8	1
Area of T_{B11}< 210 K	-31	-11	-21	-18	14	-2
Area of T_{B11}< 235 K	-18	-8	-13	15	-7	4
Flashes	12	-38	-13	-29	45	8

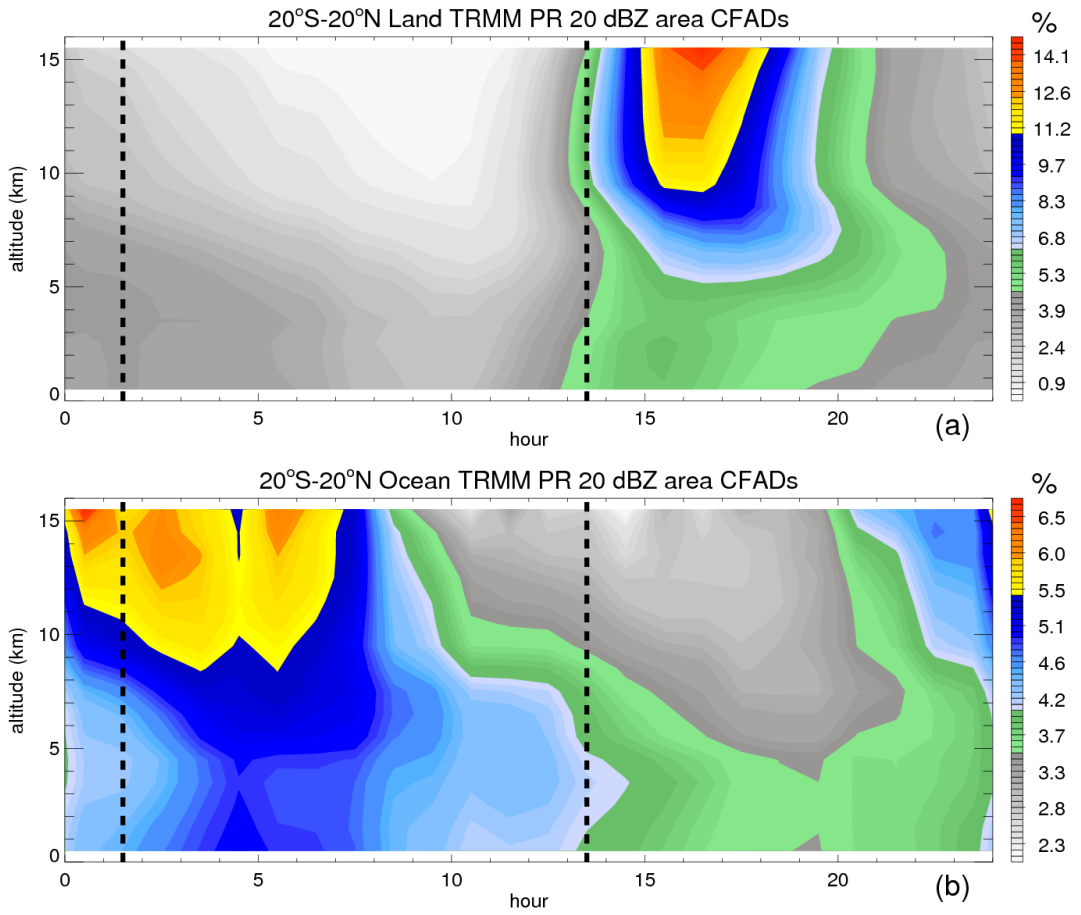

Figure 1. Contoured Frequency-by-Altitudes Diagrams (CFADs) of diurnal variation of precipitation area with TRMM PR reflectivity greater than or equal to 20 dBZ over 20°S-20°N land (a) and ocean (b). Units are in %. Vertical dashed lines are the A-Train satellite observations around 0130 and 1330 local time.

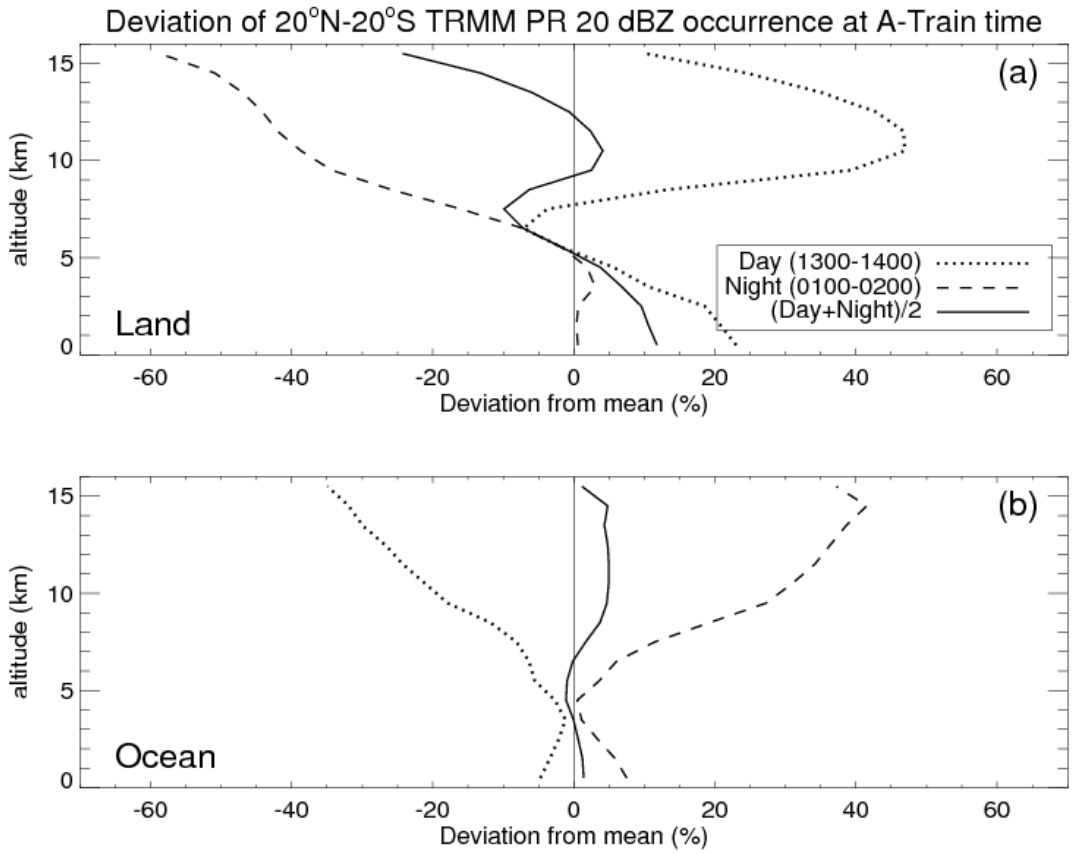

490

491 Figure 2. Percentage differences from occurrence of TRMM PR 20 dBZ around the A-

492 Train observing day time (0100-0200) and the night time (1300-1400) to the all day mean

493 occurrence over 20°S-20°N land (a) and ocean (b).

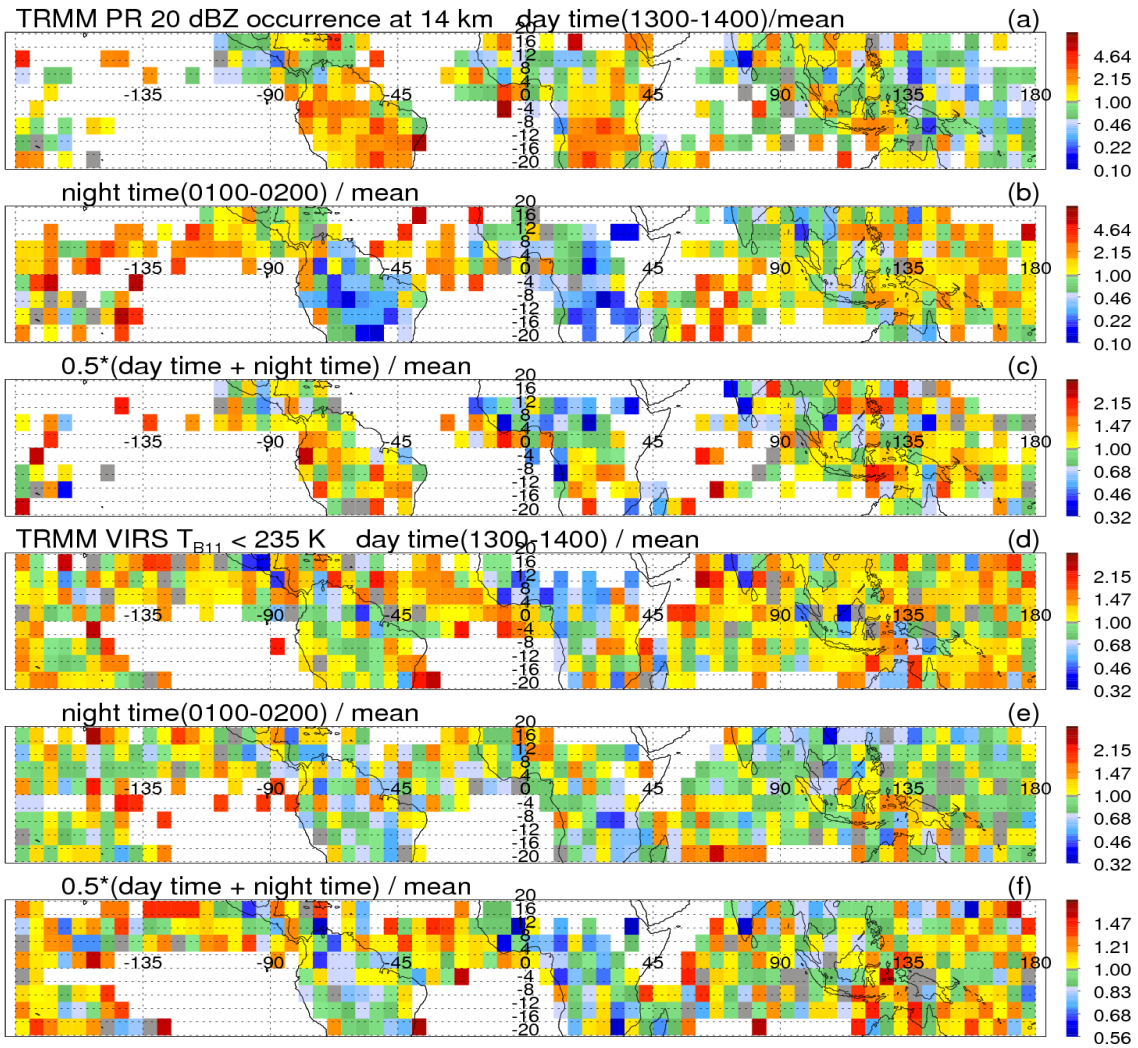

Figure 3. a) Ratio of the occurrence of TRMM PR 20 dBZ at 14 km at 1300-1400 to the mean from 9 years of full day samples, only shown for $5^{o}\times5^{o}$ boxes with at least 10 pixels with 20 dBZ. b) same as a), but for occurrence at 0100-0200. c) same as a) but for occurrence of averaging 0100-0200 and 1300-1400, only shown for $5^{o}\times5^{o}$ boxes with at least 10 pixels with 20 dBZ at both 1300-1400 and 0100-0200. d) Ratio of the occurrence of TRMM VIRS T_{B11} < 235 K at 1300-1400 to the mean from all day samples, only shown for $5^{o}\times5^{o}$ boxes with at least 10000 pixels with T_{B11} < 235 K. e) same as d), but for ratio of occurrence at 0100-0200 to the mean. f) same as d) but for ratio of occurrence of averaging 0100-0200 and 1300-1400 to the mean.

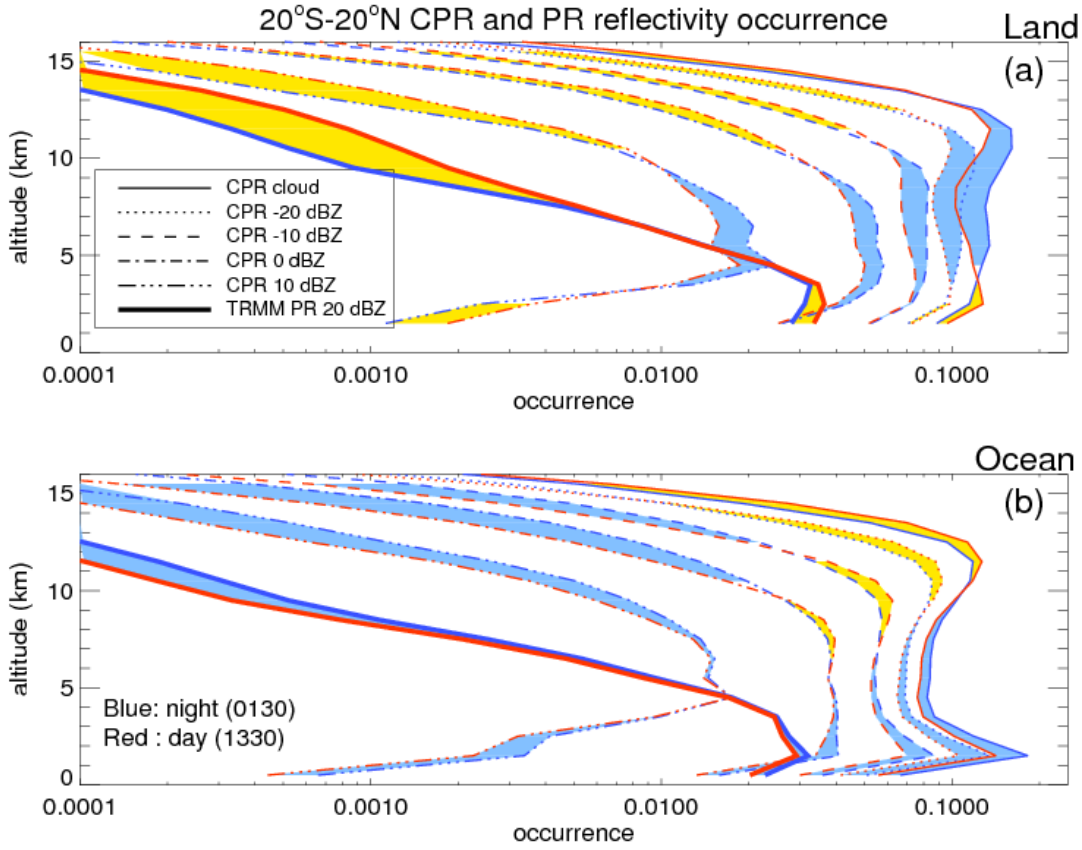

Figure 4. Occurrence (fraction) of sampled pixels with cloud mask, -20, -10, 0, 10 dBZ observed by CloudSat CPR and 20 dBZ observed by TRMM PR at different altitudes over tropical land (a) and ocean (b) (20°S-20°N) at the A-Train day (1330) and night (0130) observation times. Here TRMM PR occurrences are summarized from the observations during 0100-0200 and 1300-1400 local time. The vertical bin size is 1 km. Light blue (yellow) filled areas indicate differences when night time occurrence is greater (less) than that of day time.

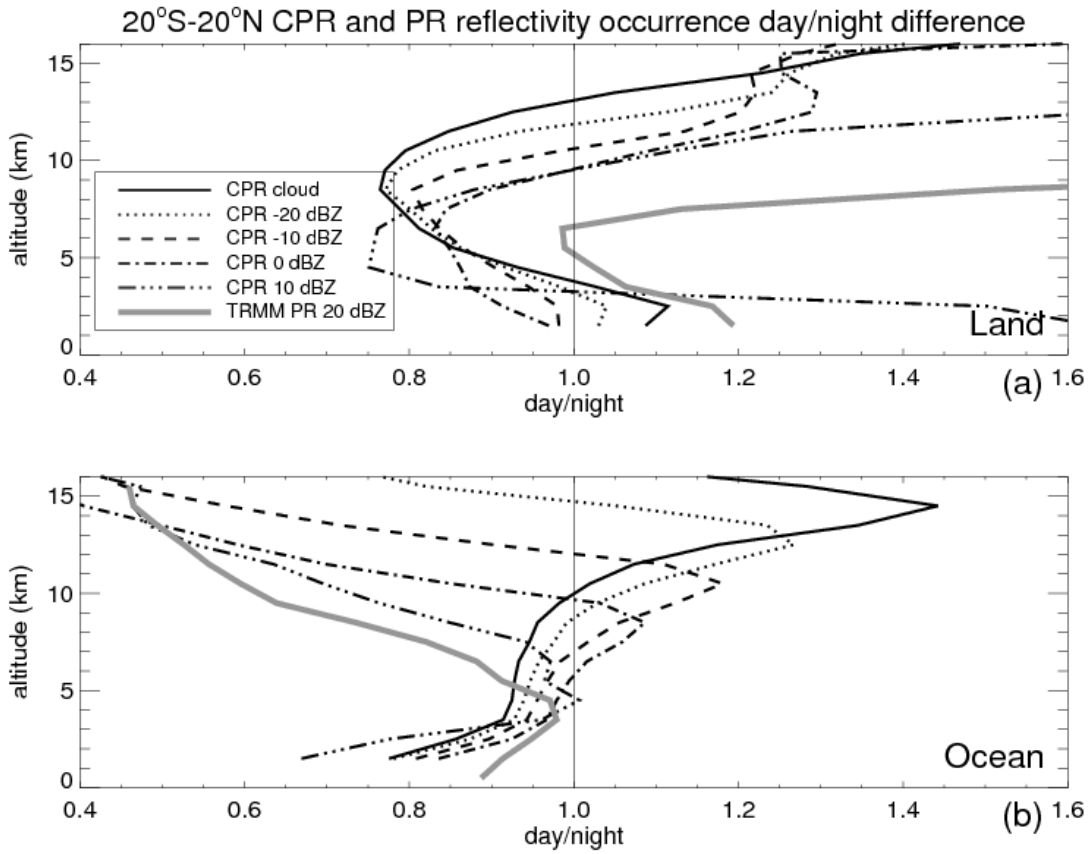

516

517 Figure 5. Ratios from the daytime to the night time CPR and PR reflectivity occurrences

518 over land (a) and ocean (b) in Figure 3.

519

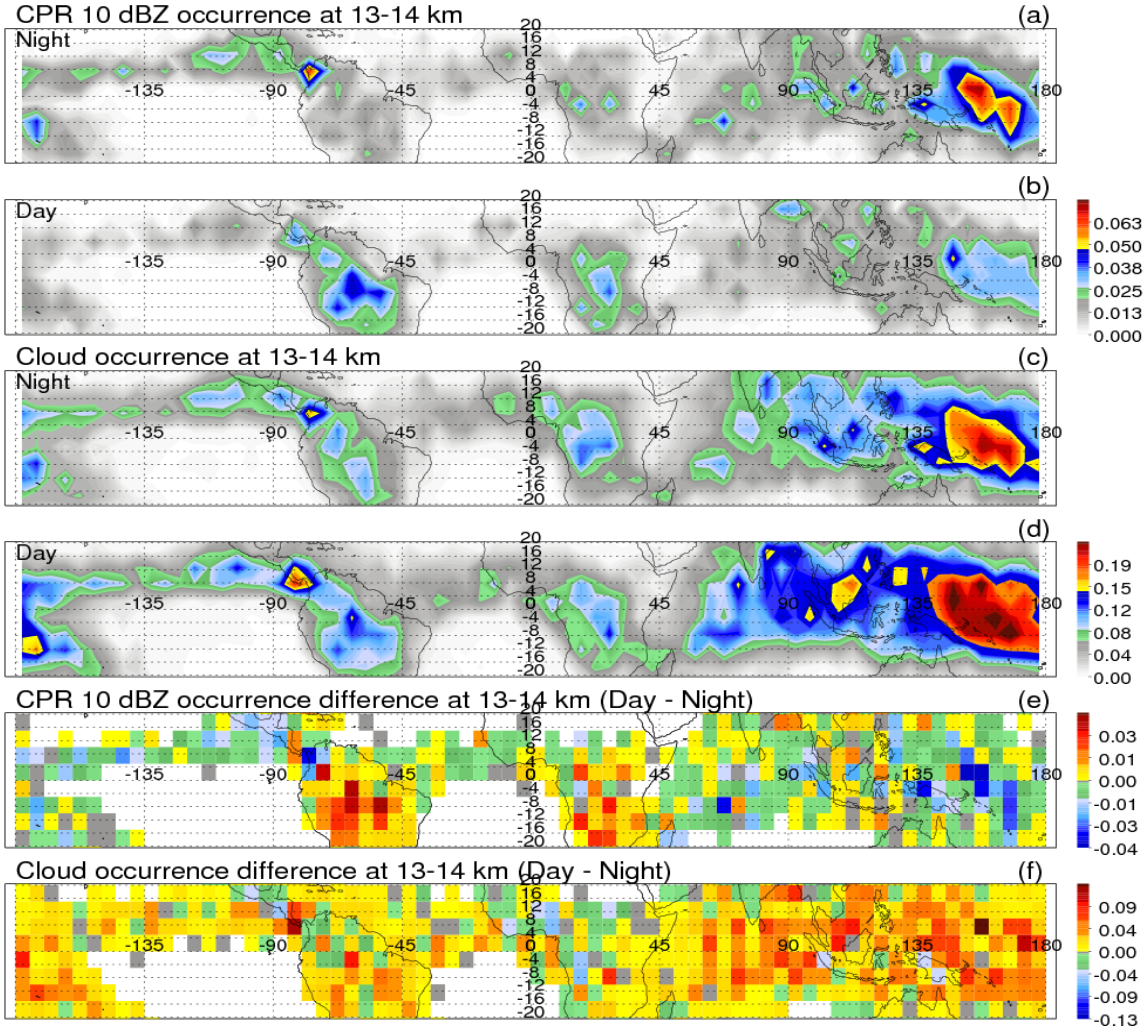

520

521 Figure 6. a) Occurrence (fraction) of CloudSat CPR reflectivity greater or equal to 10

522 dBZ at 13-14 km at night time. b) Same as a) but for day time. c) Occurrence of clouds

523 detected by CloudSat CPR at 13-14 km at night time. d) Same as c) but for day time. e)

524 Differences between day time and night time CPR 10 dBZ occurrences restricted to

525 $5^{o}\times5^{o}$ boxes with at least 1000 pixels with 10 dBZ in both a) and b). f) Differences

526 between day time and night time CPR cloud occurrences restricted to $5^{o}\times5^{o}$ boxes with at

527 least 1000 pixels with cloud mask in both c) and d).

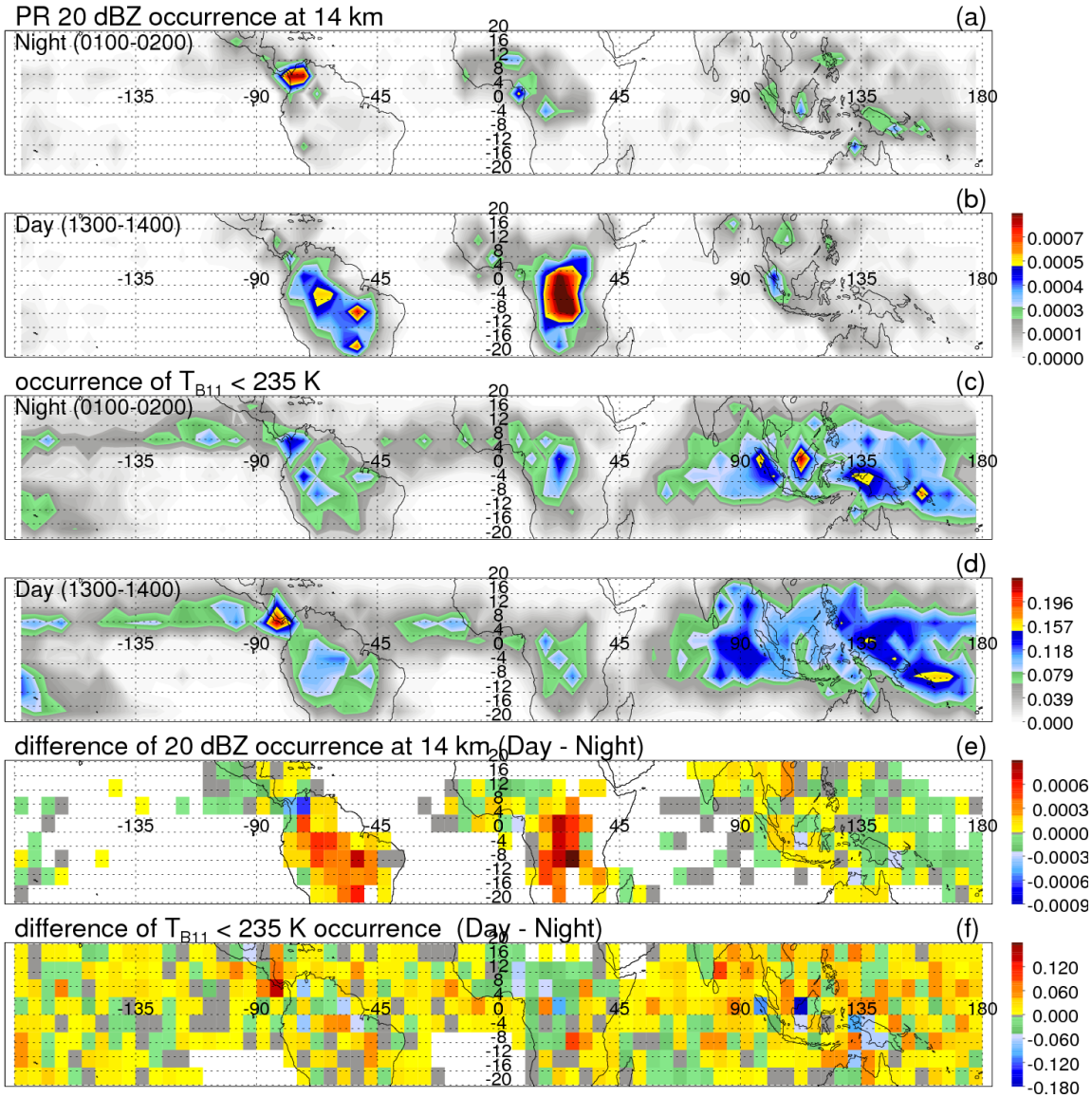

528

529 Figure 7. a) Occurrence of TRMM PR reflectivity greater or equal to 20 dBZ at 14 km for
530 night time (0100-0200). b) same as a) but for day time (1300-1400). c) Differences
531 between day time and night time. d) Occurrence of TRMM VIRS T_{B11} < 235 K for night
532 time (0100-0200). e) Differences (a)-(b) between day time and night time occurrence of
533 PR 20 dBZ at 14 km restricted to $5^{o}\times5^{o}$ boxes with at least 10 pixels of 20 dBZ in both a)
534 and b). f) Differences between day time and night time occurrence of cloud colder than

235 K restricted to $5^{o}\times5^{o}$ boxes with at least 1000 pixels of cloud colder than 235 K in both a) and b).

538

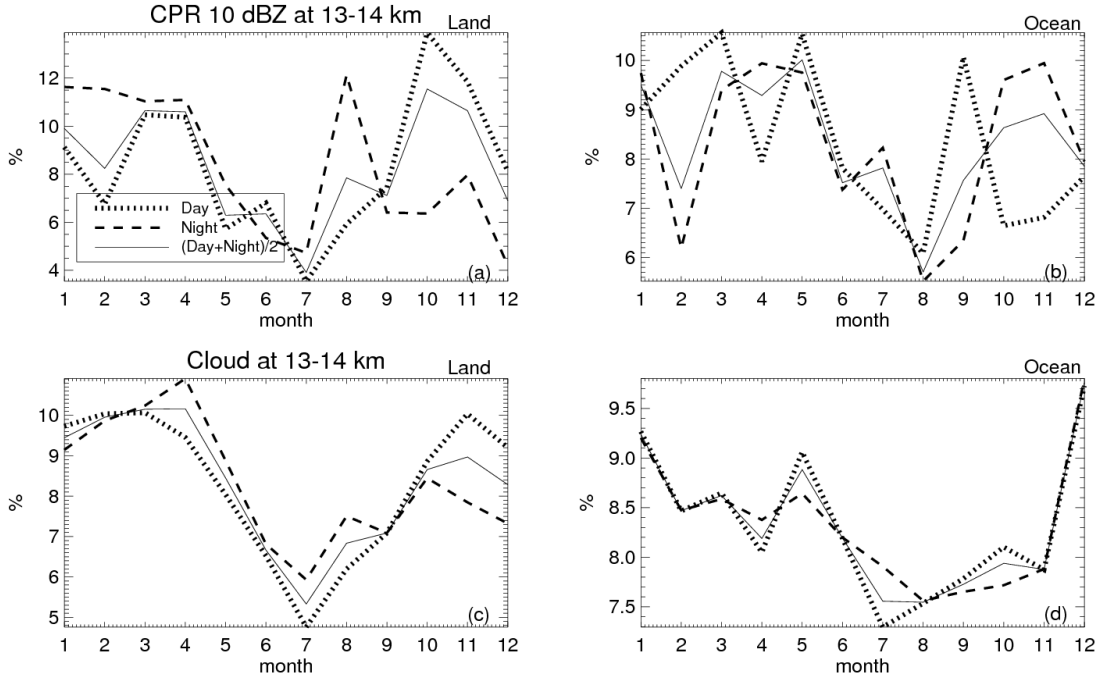

539

540 Figure 8. Seasonal variation of occurrence of CloudSat CPR clouds (c and d) at 13-14 km

541 and occurrence of CPR 10 dBZ (a and b) at 13-14 km over tropical land and ocean

542 ($20S^{o}$-$20N^{o}$). The mean values for month 1-6 are from data in 2007, and the mean values

543 for month 7-12 are from data in 2006.

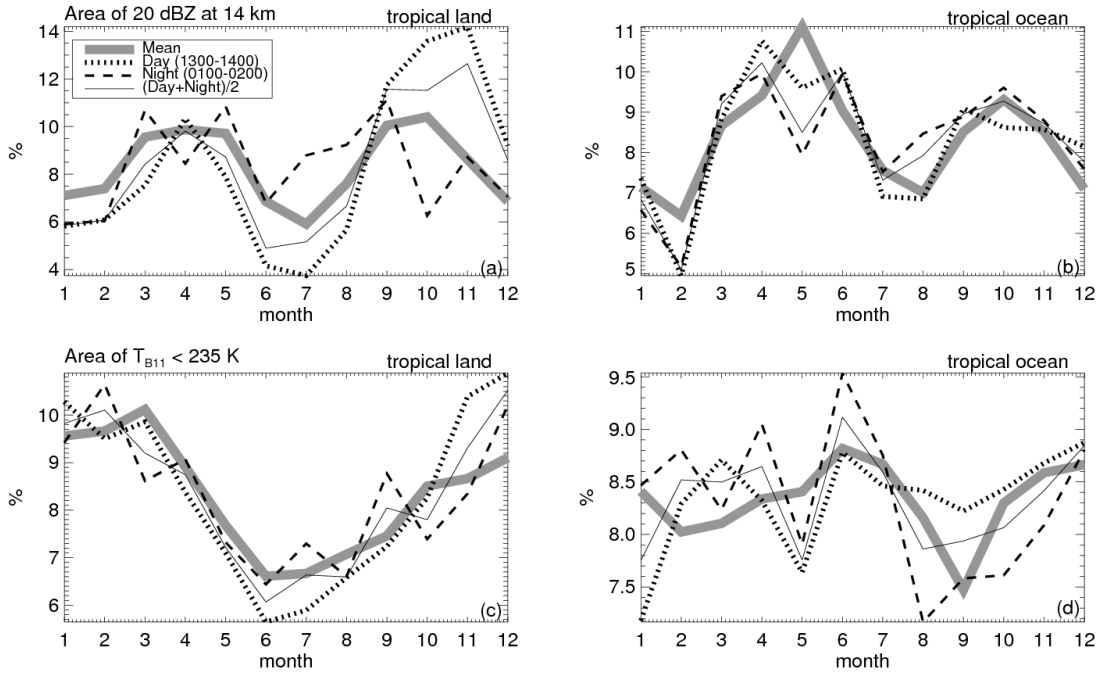

544

545 Figure 9. Seasonal variation of area of PR 20 dBZ reaching 14 km (a and b), and T_{B11} <

546 235 K (c and d) from all the TRMM observations and from only the TRMM observations

547 during 0100-0200 and 1300-1400 local time over tropical land and ocean (20^{o}S-20^{o}N).

548

548

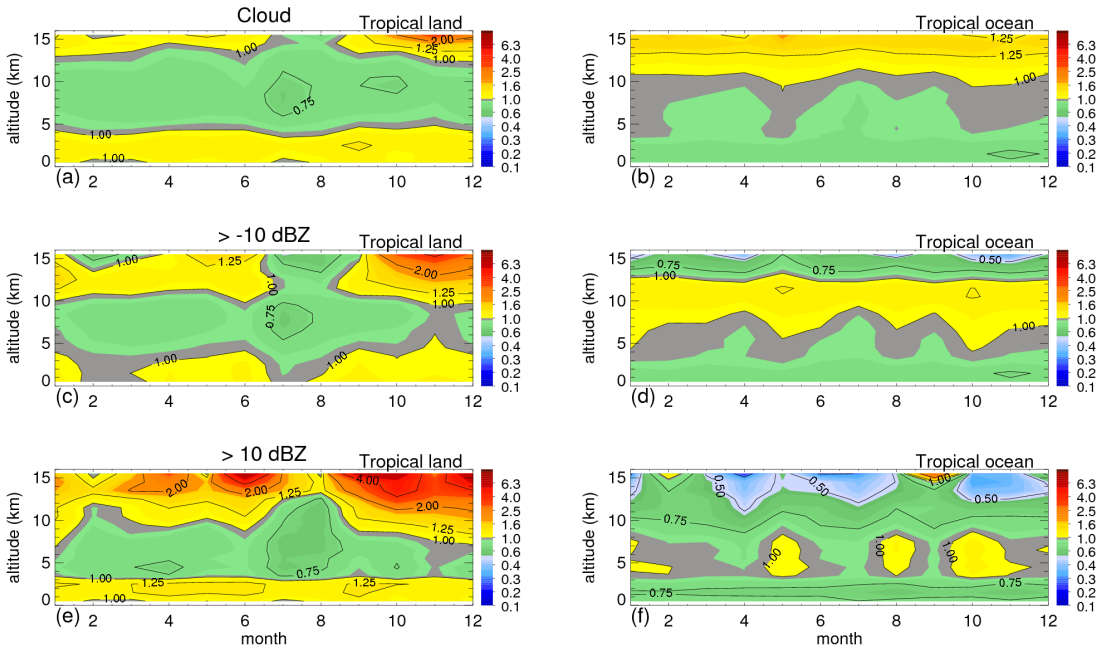

549

550 Figure 10. Seasonal variation of ratios of occurrences of CloudSat cloud, CPR reflectivity
551 > -10 dBZ, > 10 dBZ in the daytime to those at night over land and ocean. The mean
552 values for month 1-6 are from data in 2007, and mean values for month 7-12 are from
553 data in 2006.